Advances in Smart Systems Research ISSN 2050-8662
Vol. 4. No. 1 : pp.61-75 : isrp15-019

Method of Evaluating Locally Produced and Consumed Woody Biomass Resources Using Real Geographical Information: Using Satellite Images and Google Map

Yu Oya[1], Katsutoshi Kanamori[2], Hayato Ohwada[2]

[1]Department of Industrial Administration, Tokyo University of Science, Japan
7414606@ed.tus.ac.jp

[2]Department of Industrial Administration, Tokyo University of Science, Japan
{katsu, ohwada}@rs.tus.ac.jp

Abstract

Many global and environmental applications require land-use and land-cover information. There are many land-cover classifications using remote-sensing images, as they are excellent classifiers. However, this requires much training data and at least the same amount of test data. In addition, there are few classification groups because it is difficult to obtain a large amount of training data for each class. Therefore, it is also difficult to use biomass resources of unknown forests. In traditional models, so much manpower, money, and time are required to conduct field research. This study classified remote-sensing imagery for different time series by semi-supervised learning based on the maximum-likelihood method and found the location that matched other classification results. In addition, this method could classify fine and large land cover with one training sample. This paper demonstrated the feasibility of biomass resource utilization and estimated resource amounts and position, discussed the transport scenario accurately for using Google Map, and evaluated operation cost for locally produced and consumed woody biomass resources. A recursive maximum-likelihood method is proposed to consult boosting approach. It provided good performance and presented a scenario for using woody biomass resources. In future work, it will be necessary to broaden the objective area and find a relationship between vegetation condition and capital potential. On that basis, we need to research a scenario of locally produced and consumed woody biomass resources for a broad area.

1. Introduction

Many global and environmental applications require land-use and land-cover information. One such application is utilization of woody biomass resources [1]. Woody biomass has potential benefits for environmental and energy issues. Despite the large quantity of uncontrolled forest, woody biomass resources, especially tree biomass, are not used. To harness tree biomass, it is important to determine the resource distribution. However, much manpower, money, and time are required. Thus, it is necessary to develop a resource-distribution map that

indicates resource location and quantity. At present, image classification, a remote-sensing technology, is the most commonly applied approach in deriving distributed maps of land use and land cover [2]. In addition, many classification methods have been developed for classifying remote-sensing imagery; a comprehensive review of the same is given in Lu et al. [3]. One such method is unsupervised learning, but existing technology isn't considered of value for woody biomass. Unsupervised learning is good for researching land-cover changes, so it can classify cursory land use (e.g., water, urban, and vegetation) [4][5]. However, it is necessary to find tree species, location, and quantity for using biomass resources. Another such method is supervised learning, which can classify detailed land use (e.g., castanopsis live oak, cryptomeria japonica, and Japanese cypress). Here, supervised classification approaches are based on using training samples taken directly from satellite images to find spectrally similar pixels in the remote-sensing data using various statistical approaches. The approaches are the Maximum-Likelihood Method (MLM) [6], Random Forest (RF) [7], and Support-Vector Machine (SVM) [8][9]. The SVM is particularly useful in land-cover classification. In fact, many studies use an intelligent optimization algorithm. However, the definition of a proper training set is an important issue in building a classification method. In many cases, acquiring ground-truth data from a large number of training examples is expensive and time consuming, but it is easier to obtain unlabeled samples [10]. Researchers have proposed semi-supervised learning methods because of this problem [11]. However, most semi-supervised learning methods use labeled data as much as unlabeled data [12][13]. It is difficult to apply to real tasks because it is difficult to obtain land-use information in many cases. In contrast, many studies of land-cover classification make rather crude distinctions (e.g., water, soil, and forest). There are many uncontrolled forest areas, and it is difficult to refer to an unspecified forest to manage and conserve forests, utilize the resources of woody biomass, and so on. Because there is no forest registration, classification methods cannot learn without many training samples.

The objective of this study is thus to evaluate the self-training data from one training sample and demonstrate that this method is useful for estimating the location and quantity of woody biomass resources.

In this proposal, we classified remote-sensing imagery for different time series and found the location that matched other classification results by MLM. This is one of the most popular land-cover classification methods and is able to classify land using a small number of samples if the number of samples exceeds the number of attributes. Under this assumption, we selected Landsat 8 as our source of satellite images because it provides low-spectral images in eleven bands, and the images record the reflectance ratios of specific wavelengths. In general, hyper-spectral images were used for land-cover classification [14].

We then classified bundling time series images using the results regarded as training data because they might have right answer potential. Here, bundling means regarding several images as an aggregate. This was performed many times to determine how to randomly sample self-training. We observed the results. In addition, we obtained different results by combining multi-supervised learning. New self-training was then created based on the results as before. This study used 12

classes to make a detailed land-use map. The approach can be repeated until the amount of self-training data is stable. This method was thus able to achieve high-precision self-training based on a few samples. We believe that this is an excellent image-classification method.
In addition, we evaluated locally produced and consumed woody biomass resources using these classification results; we then discussed the transport scenario. To estimate the forest growth increment, trees were cut, transported to a nearby power generation plant, dried before co-combustion, and produced energy [15-18].
This paper is organized as follows. Section 2 presents a theory of land-cover classification and a proposed image-classification method involving machine learning and use of time-series data. It also describes how to transport and harness resources to evaluate woody biomass use. Section 3 reports the experiment results and discusses a comparative study, and Section 4 provides our conclusions.

2. Method

This section presents the method of evaluating locally produced and consumed woody biomass resources with real geographical information. Here, we use satellite images as remote-sensing data and Google Maps as a map search service. This paper therefore shows how to obtain tangible data and estimate resource potential for a given region. Specifically, this method includes three parts: (1) classifying land cover using satellite images, (2) predicting resource amount and position using classification results, and (3) estimating transport cost using Google Maps.

2.1. Land Cover Classification

Land-cover classification determines the class at a given location using remote-sensing data. It then uses spectral-reflectance characteristics. This spectrum includes several light wavelengths such as visible (e.g., blue, green, and red), near infrared, and middle infrared. A satellite image records reflectance as a particular bit of wavelength band; remote-sensing data includes several images of every band. In addition, a physical body has specific reflectance characteristics. Therefore, land-cover classification employs spectral reflectance characteristics. This classification thus looks for similar characteristics for water, loam, trees, and so on.
This study classifies satellite images using the Maximum-Likelihood Method (MLM). It is one of the most popular techniques for land-cover classification and is defined in the following equation [19].

$$f_k(x) = ln|\Sigma_k| + (x - m_k)^T {\Sigma_k}^{-1}(x - m_k) \quad (1)$$

Equation (1) uses a discriminant function. MLM calculates the discriminant functions $f_k(x)$ and determines the class using k of the minimum $f_k(x)$. Here, variable x is the observed data, constant k is the classification group, variable m_k is a mean vector, and variable Σ_k is a variance-covariance matrix of class k. The elements of MLM are calculated as follows. An observed datum x is a one-dimensional vector consisting of bands at a location. Mean vectors m_k and variance-covariance matrixes Σ_k are vector spaces. They are composed of training data x. In order to use the correct data, MLM calculates the vector spaces of m_k and Σ_k using area data randomly selected from each classification group.

In this study, there is only one training sample for each classification group. In addition, locations around the training position are regarded as having the same land cover. Therefore, a certain category has correct data of nine pixels. However, this classification will be less accurate because there are few training data even if machine learning is used. In fact, Random Forest had high training accuracy but low test accuracy. We propose ensemble learning by time series remote-sensing data. This classification technique includes two steps: (1-A) ensemble group MLM for each season and (1-B) recursively ensemble MLM by boosting.

In step 1-A, this technique requires several satellite images acquired at different times. We selected the four seasons from spring to winter for the time series remote-sensing data because different seasons have different remote-sensing data (e.g., deciduous trees have leaves in summer, but not in winter). On that basis, positions having same classification results of MLM has high potential as alternatives to training data. This method classifies satellite images four times for each season by MLM and finds locations having common results. These could be right. We regard places receiving the same labels in results as correct data, and these are made available for training samples. Fig. 1 left describes this flow. This approach maximizes supervised learning with few samples. However, MLM cannot calculate a result when there are fewer samples than attributes; it is the number of bands (images) in this instance. Therefore, a season should have fewer than nine attributes.

In step 1-B, the existing approaches require much training data. Step 1-A might not have enough correct data to work with. Therefore, this technique increases the number of training samples by using recursion algorithms as illustrated in Fig. 1 right. MLM classifies all of the satellite images. If this continues, there is only one result. This method uses several training data sets sampled randomly from previous results and classifies the data-bundled images for each created training dataset. This method is thus able to classify by MLM over and over again. After learning several times, ensemble learning is able to produce a final classification result. In addition, isolated land cover (e.g., trees enclosed by water) is regarded as same that surrounding land cover class just like a life game because they may be in error.

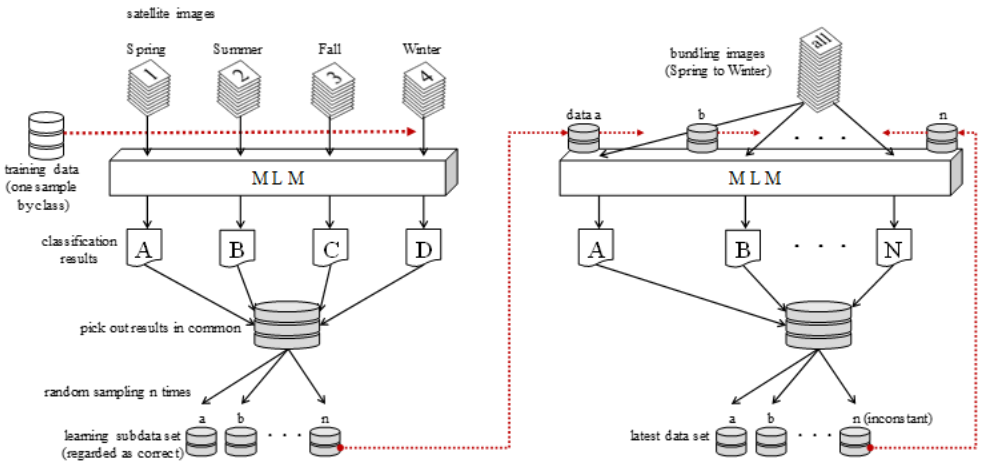

Fig. 1. Proposed technique (Left: First step. Right: Second recursive step.)

2.2. Estimating Resources and Position

This study estimates woody biomass resources and positional information using the results of land-cover classification. No study estimates the resource quantity of woody biomass. This paper demonstrates that it is easy to calculate resource use. This method regards the annual allowable resource as forest increments. Woody biomass resources are thus less than the amount of forest growth. Based on this idea, this method calculates wood-cover area (number of pixels), forest growth, and woody biomass resources using the following equation.

$$W = (\mu + 1.96\sigma \times NDVI) \times I \times S \quad (2)$$

Equation (2) estimates the forest increment for the year. It needs to numerate forest-cover pixels based on classification results and convert them to the real wood-cover area. Variable S is the wood-cover area. S is covered with a certain land cover. It's the product of pixels and the square of resolution performance, with square meters converted to hectare. Here, a pixel is included area of square resolution performance. Variable I is a forest increment coefficient depending on land-cover class. The forest growth is thus calculated using the relationship between wooded area and volume. The two columns on the left of Table 1 indicate the timber volume per hectare. In addition, wood volume is transformed to mass using tree columns of Table 1 on the right because we need mass, not volume. However, wood mass depends on its density even for the same area or volume. Therefore, we use the Normalized Difference Vegetation Index (NDVI) [20]. Here, NDVI has the advantage of a correlated band in the classification of trees because it indicates the activation level of vegetation. NDVI provides the difference between wavelengths of near-infrared band (NIR) and visible red band (R). Equation (3) calculates the difference.

$$NDVI = \frac{(NIR - R)}{(NIR + R)} \quad (3)$$

Wood mass is assumed to have a normal distribution with median μ and standard deviation σ of Table 1, with a confidence level of 95%. NDVI of Eq. (3) ranges from -1.0 to 1.0; thus, this method regards NDVI as an indicator of deviation from the average value μ: the higher the NDVI, the more resources. For these reasons, this method estimates woody biomass resources based on real wood-cover area S in hectares. In addition, this paper defines energy contained in woody biomass as in the following equations.

$$W' = 0.5W \text{ [kg-dry/yr]} \quad (4)$$

$$E = 45.71 \times 0.5W' - 2.70 \text{ [MJ-HHV/kg-dry]} \quad (5)$$

Equation (4) calculates the dry measure of woody biomass for 100% moisture content. Equation (5) estimates the energy amount when there is half carbon content in dry measure W. This method conforms to the following protocol.

1. Transport resources W to nearby power-generating plants.
2. Dry resource from 100% water content to 25%.
3. Generate electricity by co-combustion.

In step (2), this paper hypothesizes that the vaporization heat of water is 2,512 kJ/kg, the combustion efficiency ratio of the boiler is 80%, and the energy to dry is 1,177.5 kJ/kg. In addition, the energy is provided by generated electricity from biomass. Here, the co-combustion efficiency is 33% and 0.27778 kWh/MJ.
A woody biomass location is calculated by the area S. We are able to obtain the coordinates of the center of gravity in S according to the criteria of the upper-left plane coordinates of Universal Transverse Mercator (UTM) because resolution is width or height per 1 pixel. Plane coordinates of the center are transformed to geographical coordinates in latitude and longitude.

Species	volume [m^3/ha/yr]	mass [kg/m^3]		
	I	range	μ	σ
Conifer	6.2	262.6 - 574.5	418.6	79.6
Broadleaf tree	1.2	470.1 - 829.9	650.0	91.8

Table 1. Relationship between wooded area, volume and mass

2.3. Evaluation of transporting and harnessing resource

After this method finds woody biomass resources and positional information, it evaluates locally produced and consumed woody biomass resources to estimate the total cost when resources are transported from forests to power-generating plants. This study regards transport cost as machine, fuel, and manpower for tree trimming, timber collecting, operation (e.g., chipping and bundling), and transport. Table 2 lists equations for estimating cost.

Species	Machine	Estimate Equation [yen/1000kg-dry]
Conifer	forestry tractor	$2.11L_{SY} + 0.068L_T + 229e^{0.117d} + 11408$
	timber collecting	$1904\,{L_{SY}}^{0.2142} + 31023\,{L_T}^{-1} + 0.068L_T + 8518$
Broadleaf	forestry tractor	$1.58L_{SY} + 0.048L_T + 164e^{0.117d} + 8371$
	timber collecting	$1360\,{L_{SY}}^{0.2142} + 22159\,{L_T}^{-1} + 0.048L_T + 6307$

Table 2. Equations for estimating transportation cost

In table 2, L_{SY} is the distance of transporting timber from the forest to the nearest road, L_T is the distance to nearby thermal power plants, and d is the terrain slope. We can obtain this information through Google Maps and resources positional coordinates.

3. 3. Experiment

This section presents experiments to demonstrate the usefulness of this method. We developed land-cover classification and estimated woody biomass resources with the addition of location information using MATLAB, numerical software that enables digital-image processing.

3.1. Dataset

Practical applications should classify unknown regions. This study looks into the usefulness of these methods. Our target region was Kamakura City, Kanagawa Prefecture, Japan, for which much land-cover information is known. This paper sets up as many classification groups as possible in order to make a fine vegetation map consisting of 12 categories. Here, we utilized a land-use map that the Ministry of the Environment made on foot in 2000 to manage and conserve forests as truth data to enhance classification accuracy. Fig. 2 shows the land-use map of right answer data. In addition, we determined the correct land-cover of a certain location for each classification group and regarded the eight surrounding pixels of training data as the same class. These training positions were sampled at random for each class.
Second, we selected correlated bands from Landsat 8, an artificial satellite launched in 2013. Its satellite images are not hyper spectral images but coarser multispectral images. Dube et al. evaluated the utility of Landsat 8 for quantifying

aboveground biomass in South Africa [21]. The satellite image, called a "band," records the reflectance ratios at various wavelengths. In Landsat 8, Operational Land Imager (OLI) and Thermal Infrared Sensor (TIRS) images consist of nine spectral bands with a spatial resolution of 30 meters for Bands 1 to 7 and 9. Thermal Bands 10 and 11 are useful in providing more accurate surface temperatures and are collected at 100-meter intervals. Here, we can use less than nine bands because there is only nine training data for a certain class. Therefore, within a given classification group, we found the band-to-band relations and avoided using unrelated bands in all groups. As a result, we selected Bands 1 to 3 and 7. In addition, we used remote-sensing data without clouds acquired on September 1, 2013 (summer), November 20, 2013 (fall), January 23, 2014 (winter), and May 22, 2014 (spring).

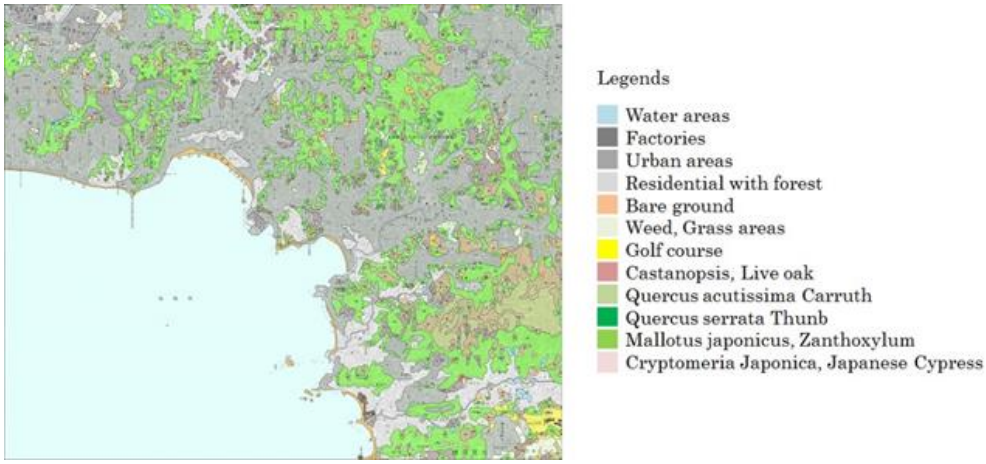

Fig. 2. Land-use map as right data

3.2. Experiment

Basically, we conducted experiments in accordance with this method. First, we classified an object region using satellite images and four bands selected by MLM. We were able to obtain four classification results, one each for spring, summer, fall, and winter, and we found points with the same class among the results. We thus regarded the classification results to have the right potential as training samples. Second, we classified a target region using all images, analyzing 16 attributes several times by MLM. Here, the training samples and attributes were sampled randomly from previous results for each running classification. We were able to obtain several classification results for each trial. We then found the common points, determined which were positive, and made new training samples as before. This method can be employed many times. This operation was repeated until there were training samples for about half of the target region. Third, we segmented the final classification result for each object having the same class on vegetation area.

Here, we ignored small objects with fewer than 50 pixels. In addition, we estimated the biomass resource amount and positions. The coordinates of positions are latitude and longitude of an object centroid.

3.3. Evaluation methodology

To evaluate the classification precision, we made a confusion matrix and worked out the Kappa coefficient during the verification process [22]. The Kappa coefficient is calculated using the following equation.

$$\kappa = \frac{\sum w_{ii} - \sum(w_{i*}w_{*i})}{1 - \sum(w_{i*}w_{*i})} \quad (6)$$

Here, w_{ki} represents the elements in the confusion matrix, and the weight of expected class i in observed class k. When the diagonal cells contain weights of 0 and all of the off-diagonal cells contain weights are 1, this formula produces the same value of kappa as the above calculation. The Kappa coefficient is generally considered to be a more robust measure than a simple percent-agreement calculation since it takes into account the agreement occurring by chance. According to Landis et al. [23], a Kappa coefficient less than 0 indicates no agreement, 0 to 0.20 as slight agreement, 0.21 to 0.40 a fair agreement, 0.41 to 0.60 a moderate agreement, 0.61 to 0.80 a substantial agreement, and 0.81 to 1 an almost perfect agreement.
To evaluate transport cost, we compared between our result and a following case of setup coefficients in Table 2. L_{SY} is the average distance from the centroid to the circumference of a resource object, L_T is 1.5 times the straight-line distance between resource positions and power plant locations, and d is 15 degree. This was often used as a model case in previous works.

3.4. Experiment Results

Table 3 indicates the confusion matrix between the land-use map depicted in Fig. 2 and the final classification result shown in Fig. 3. In Table 3, the rows are the correct groups, the columns are the classification result groups, the elements are the number of pixels, and the diagonal elements are the correct classification. This method had the results described above. In the final classification trial (10 times), the self-training samples covered 82.1% of the object region. The classification results were as follows: the simple percent agreement was 71.6% and Kappa coefficient was 0.644. This was much better than the other learning methods (e.g., Random Forest and Support-Vector Machine) because there was little training data. Therefore, this method has potential for regions around the globe without land-use maps.

Fig. 3. Result of land-cover classification

		Expected class											
		1	2	3	4	5	6	7	8	9	10	11	12
Observed class	1	39046	0	0	87	9	3	0	0	4	0	0	0
	2	37	1227	0	0	23	138	238	13	31	129	3	51
	3	431	0	24311	0	98	345	55	161	362	1313	131	436
	4	26	0	0	4677	13	35	1	17	42	112	19	49
	5	931	307	688	197	630	0	0	17	69	65	46	56
	6	58	130	1086	400	0	846	0	32	31	200	21	29
	7	45	82	656	446	0	0	460	59	41	250	50	114
	8	252	469	3183	1392	93	361	78	3972	224	5053	461	1164
	9	320	54	792	344	18	49	14	47	522	309	24	175
	10	3	141	327	175	22	50	23	189	39	4035	237	456
	11	9	71	243	113	14	31	51	199	17	1954	1654	829
	12	3	49	327	63	22	40	18	122	24	1557	452	2268

Table 3. Confusion matrix between land-use map

In addition, we compared the previous study by Kamagata et al. [24]. Table 4 suggests that this study had better accuracy than the previous work, although it had a larger area, coarser images, and more classes. The objective of this study is to estimate correct data from classification results for extracted locations with common results for many classes, so only correct data should be extracted. However, the results had many errors, meaning that the training data might not be robust enough to use the existing land-cover classification. This method offers the possibility of increasing the number of training samples until a full cover ratio is reached. The problem is the amount of time required for classification because this method performs supervised learning over and over again. Therefore, this method

should be optimized to decrease the amount of calculation. Table 5 presents the results for the resource being transported to Minami-Yokohama power-generating plant or Yokosuka thermal electric power station in Fig. 4.

	Kamagata et al.	This study
Target area	Kamakura	Kamakura
Region	Mountainous	plain
Area	25 km^2	102,724 km^2
Training data	too much	12 pixels
Satellite image	IKONOS	Landsat 8
Spatial resolution	4 m	30 m
Number of classes	7	12
Kappa coefficient	0.526	0.644
Degree of coincidence	moderate	substantial

Table 4. Comparison with previous work

Total resources quantity	858,229.22	kg
Generated energy	10,615,017.22	MJ-HHV
Drying energy	1,010,564.91	MJ
Electricity generated	618,305.21	kWh
Transport costv	10,615,017	JPY
Unit cost	17.168	JPY/kWh

Table 5. Results of transport scenario

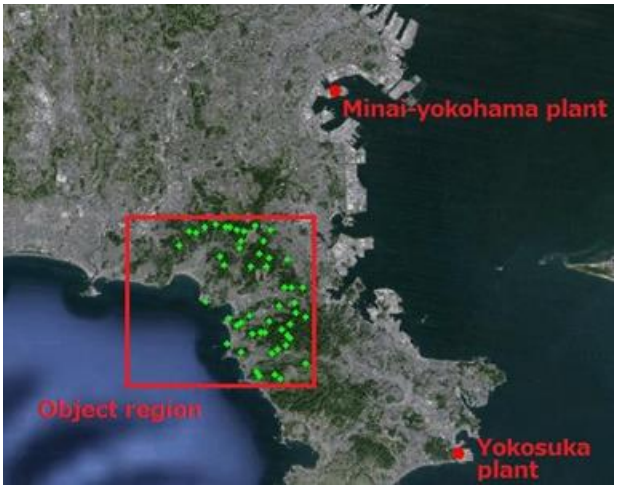

Fig. 4. Resource distribution map and power plant

This scenario is actual costs without destruction of natural resources. In addition, the electric generating capacity is equivalent to the usage of 172 family units and 2.88% of the people in Kamakura City. Biomass resources are expensive because of transport, so locally produced and consumed resources is the optimum approach for biomass. However, there is an inverse relationship between the amount of resources and population: regions using a lot of electricity produce little electric power. Thirty percent of the target region is vegetation area, leading to a better balance between supply and demand. In future works, we should search for the relation between the forest cover ratio and biomass resource utility.
In Fig. 5, the horizontal axis is the theoretical value of 1.5 times the straight-line distance, and the vertical axis is measured using Google Maps route search. We can see that it was difficult to predict transportation distances less than 25km by linear regression. The error is small in this scenario. In fact, there is a 0.1% error of transportation cost between the observed distance and the theoretical distance. However, this scenario was a small model, and the object region covered 0.2% of the satellite images. Therefore, we are not able to tolerate margins of this error because we could experiment this method for 500 times larger object area if we checked a little land cover for training.

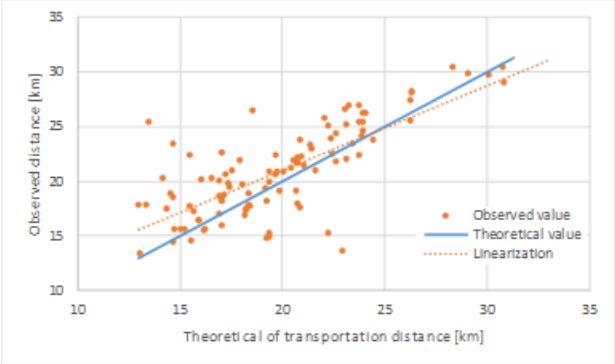

Fig. 5. Transport distance relation between observed and theoretical distance

4. Conclusion

This study employed real geographical information to evaluate the capabilities of locally produced and consumed woody biomass resources. One bit of geographical information is land cover. We proposed a recursive maximum-likelihood method and consulted the boosting approach. This method classified time-series satellite images and had fine results for more than comparable areas without much training data. Another bit of geographical information is the transport route. We estimated the transportation cost using observed distances on Google Maps. This approach enabled us to evaluate the woody biomass resource amount, positional information, transport distance, and cost.

Today, many global and environmental applications require land-use and land-cover information. Many land-cover classifications use remote-sensing images, as they are excellent classifiers. However, this requires a lot of training data and at least the same amount of test data. In addition, they have few classification groups because it is difficult to obtain a large amount of training data for each class. Therefore, it is difficult to use biomass resources of unknown forest. In traditional models, so much manpower, money, and time are required to conduct field research. This study was able to classify many areas and select locations that were potentially correct. This paper thus demonstrates the feasibility of biomass resource utilization by resource amount and position. In future work, it will be necessary to broaden the objective area and find a relationship between vegetation condition and capital potential. On that basis, we need to research a scenario of locally produced and consumed woody biomass resources for a broad area.

5. References

[1] Hans-Erik A., Jacob S., Hailemariam T., Donald A., and Ken W., Using multilevel remote sensing and ground data to estimate forest biomass resources in remote regions: a case study in the boreal forests of interior Alaska, Canadian Journal of Remote Sensing, 37(6): 596-611, 2012.
[2] Zhe Zhu, and Curtis E. Woodcock, Continuous change detection and classification of land cover using all available Landsat data, Remote Sensing of Environment, 114: 152-171, 2014
[3] Lu D., and Weng Q., A survey of image classification methods and techniques for improving classification performance. International Journal of Remote Sensing, 28(5): 823-870, 2007.
[4] Matthew C. Hansen, and Thomas R. Loveland, A review of large area monitoring of land cover change using Landsat data, Remote Sensing of Environment, 122: 66-74, 2012.
[5] Banerjee B., Bovolo F., Bhattacharya A., and Bruzzone, L., A New Self-Training-Based Unsupervised Satellite Image Classification Technique Using Cluster Ensemble Strategy, Geoscience and Remote Sensing Letters, 12(4): 741-745, 2015
[6] Alan H. Strahler, The use of prior probabilities in maximum likelihood classification of remotely sensed data, Remote Sensing of Environment, 10: 135-163, 1980.
[7] V.F. Rodriguez-Galiano, B. Ghimire, J. Rogan, M. Chica-Olmo, and J.P. Rigol-Sanchez, An assessment of the effectiveness of a random forest classifier for land-cover classification, ISPRS Journal of Photogrammetry and Remote Sensing, 67: 93-104, 2012.
[8] Vapnik V.,. The Nature of Statistical Learning Theory, Springer-Verlag, New York, 1995.
[9] Pal M., and Mather P.M., Support vector machines for classification in remote sensing, International Journal of Remote Sensing, 26(5): 1007-1011, 2005.

[10]Foody G.M., and Mathur A., The use of small training sets containing mixed pixels for accurate hard image classification: training on mixed spectral responses for classification by a SVM, Remote Sensing of Environment, 103(2): 179-189, 2006.
[11]Ghoggali N., and Melgani F., Genetic SVM approach to semisupervised multitemporal classification, IEEE Geoscience and Remote Sensing Letters, 5(2): 212-216, 2008.
[12]Maulik U., and Chakraborty D., A self-trained ensemble with semisupervised SVM: an application to pixel classification of remote sensing imagery, Pattern Recognition, 44: 615-623, 2011.
[13]Ying L., Bai Z., Limin W., and Nan W., A self-trained semisupervised SVM approach to the remote sensing land-cover classification, Original Research Article Computers & Geosciences, 59: 98-107, 2013.
[14]Omar Benarchid, and Naoufal Raissouni, Potential of Semi-automatic Object-based Land Cover Classifications using Very High Resolution Satellite Images: Tetuan-city Comparison Case Study, Journal of Space Science & Technology, 2(3): 19-28, 2013.
[15]M. Iuchi, Development of the support system for biomass energy business plans -The data base and evaluation models to simulate the collection cost-, Central Research Institute of Electric Power Industry Report, Y03023, 2004.
[16]T. Kinoshita, K. Inoue, K. Iwao, H. Kagemoto, Y. Yamagata, A spatial evaluation of forest biomass usage using GIS, Applied Energy, 86: 1-6, 2009.
[17]H. Yamamoto, T. Nakata, K. Yabe, Design of Biomass Co-firing System Considering Resource Distribution and Transportation Optimization, Journal of Japan Institute of Energy, 89: 42-52, 2010.
[18]K. Moriguchi, Y. Suzuki, J. Gotou, H. Inatsuki, T. Yamagushi, Y. Shiraishi, T. Ohara, Cost of Commination and Transportation in the Case of Using Logging Residue as Woody Biofuel, Japanese Forestry Society, 86: 121-128, 2004.
[19]M.J. Canty, Image Analysis, Classification and Change Detection in Remote Sensing: with Algorithms for ENVI/IDL, CRC Press, 2007.
[20]Jiarui Dong, Robert K. Kaufmann, Ranga B. Myneni, Compton J. Tucker, Pekka E. Kauppi, Jari Liski, Wolfgang Buermann, V. Alexeyev, Malcolm K. Hughes, Remote sensing estimates of boreal and temperate forest woody biomass: carbon pools, sources, and sinks, Remote Sensing of Environment, 84: 393-410, 2003.
[21]Timothy Dube, and Onisimo Mutanga, Evaluating the utility of the medium-spatial resolution Landsat 8 multispectral sensor in quantifying aboveground biomass in uMgeni catchment, South Africa, ISPRS Journal of Photogrammetry and Remote Sensing, 101: 36-46, 2015
[22]Russell G. Congalton, A review of assessing the accuracy of classifications of remotely sensed data, Remote Sensing of Environment, 37: 35-46, 1991.
[23]J. Richard Landis, and Gary G. Koch, The Measurement of Observer Agreement for Categorical Data, Biometrics, 33: 159-174, 1977.
[24]Noritoshi Kamagata, and Keitarou Hara, Vegetation mapping by objectbased image analysis: evaluation of classification accuracy and boundary extraction

in a mountainous region of central Honshu, Japan, Vegetation Science, 27:83-94, 2010.